From twitch to tetanus for human muscle - experimental data and model predictions for m. triceps surae

van Zandwijk, J.P.; Bobbert, M.F.; Harlaar, J.; Hof, A.F.

published in
Biological Cybernetics
1998

DOI (link to publisher)
10.1007/s004220050464

document version
Publisher's PDF, also known as Version of record

Biol. Cybern. 79, 121–130 (1998)

Biological Cybernetics

From twitch to tetanus for human muscle: experimental data and model predictions for m. triceps surae

J.P. van Zandwijk[1], M.F. Bobbert[1], J. Harlaar[2], A.L. Hof[3]

[1] Institute for Fundamental and Clinical Human Movement Sciences, Faculty of Human Movement Sciences, Vrije Universiteit, Van der Boechorststraat 9, 1081 BT Amsterdam, The Netherlands
[2] Department of Rehabilitation Medicine, Free University Hospital, Amsterdam, The Netherlands
[3] Department of Medical Physiology, University of Groningen, Groningen, The Netherlands

Received: 10 November 1997 / Accepted in revised form: 26 March 1998

Abstract. In models describing the excitation of muscle by the central nervous system, it is often assumed that excitation during a tetanic contraction can be obtained by the linear summation of responses to individual stimuli, from which the active state of the muscle is calculated. We investigate here the extent to which such a model describes the excitation of human muscle in vivo. For this purpose, experiments were performed on the calf muscles of four healthy subjects. Values of parameters in the model describing the behaviour of the contractile element (CE) and the series elastic element (SEE) of this muscle group were derived on the basis of a set of isokinetic release contractions performed on a special-purpose dynamometer as well as on the basis of morphological data. Parameter values describing the excitation of the calf muscles were optimized such that the model correctly predicted plantar flexion moment histories in an isometric twitch, elicited by stimulation of the tibial nerve. For all subjects, the model using these muscle parameters was able to make reasonable predictions of isometric moment histories at higher stimulation frequencies. These results suggest that the linear summation of responses to individual stimuli can indeed give an adequate description of the process of human muscle excitation in vivo.

1 Introduction

Forward dynamical modelling and simulation of the human musculo skeletal system is an effective approach to study questions in the field of multi-segment movement control. In simulation studies, muscle models, which are mathematical representations of muscle behaviour, are used to drive models of the skeleton. Usually, each muscle is represented by two separate sets of equations, one describing its contractile behaviour, the other describing its excitation by the central nervous system. The former is often called the contraction dynamics of the muscle model, the latter its excitation dynamics. In order to be able to answer questions concerning the control of movement, it is obviously important that the properties of the model of the human musculo skeletal system resemble those of the real system sufficiently well. For models used to simulate the push-off in vertical jumping (e.g. Pandy et al. 1990; Pandy and Zajac 1991; Van Soest and Bobbert 1993; Bobbert and Van Zandwijk 1994), it was found that the rate of force development was higher in the model than observed experimentally. As noted earlier (Van Zandwijk et al. 1996) this excessively rapid rise of force may be due to three factors: (i) the excitation dynamics used in the model are too fast; (ii) the contraction dynamics used are too fast; (iii) control signals rise too rapidly. In our studies, first-order dynamics as proposed by Hatze (1977, 1981) are used to describe muscle excitation. As explained in Hatze (1977, 1981), these dynamics are a simplification of a more complex model of the excitation of human muscle and describe the average behaviour of this model at high frequencies of stimulation. In the more complex model, it is assumed that excitation during a tetanic contraction can be obtained by the linear summation of responses to individual stimuli. Unfortunately, no experimental data are provided in Hatze (1977, 1981) to support the assumption that such an extrapolation from twitches to tetani adequately describes the process of human muscle excitation. However, it was recently shown (Van Zandwijk et al. 1996) that such an extrapolation does indeed give a good description of the processes involved in the excitation of rat isolated skeletal muscle.

The purpose of this research is, first, to investigate to what extent such a model of the excitation of muscle is able to describe the excitation of human muscle in vivo. Thus, we shall check that for each subject individually, the part of the muscle model which describes contractile behaviour closely reflects the contractile behaviour of human calf muscles. Subsequently, the parameters in the

Correspondence to: J.P. van Zandwijk
(e-mail: zandwijk@xs4all.nl, Tel.: +31-20-4448475,
Fax: +31-20-4448529)

excitation dynamics will be optimized such that the model predicts the mechanical response during an isometric twitch. Finally, we shall examine to what extent the muscle model is able to predict responses at other stimulation frequencies by comparing moment histories generated by the model to those obtained experimentally. In the second place, a comparison will be made between parameter values describing excitation and contraction dynamics obtained in this way and parameter values used previously in a model to simulate the push-off phase in vertical jumping (Van Soest and Bobbert 1993) as far as the rate of force development during an isometric contraction is concerned.

2 Methods

2.1 Muscle model

2.1.1 Contraction dynamics

Simulations of muscle contractions were performed using a model of a muscle-tendon complex (MTC), based on the classical model of Hill (1938). The model has been described extensively elsewhere (Van Soest and Bobbert 1993; Van Zandwijk et al. 1996). Briefly, it consists of a contractile element (CE), a series elastic element (SEE) and a parallel elastic element (PEE). When referring to human muscle in vivo, it is more convenient to express quantities in angular instead of linear coordinates. Therefore, in the following, forces will be expressed as moments, lengths as angles, velocities as angular velocities and so on. Figure 1 shows the arrangement of the elements with respect to each other.

CE. The behaviour of CE is governed by its moment-angle relationship, its moment-angular velocity relationship and its active state. The moment-angle relationship is described as a parabola and is determined by optimum CE angle $\varphi_{ce,opt}$[rad], maximum CE moment at optimum angle M_{max}[Nm], and the dimensionless shape parameter w, which determines the width of the CE moment-angle relationship. The CE moment-angular velocity relationship for shortening is described by the classical Hill equation:

$$\omega_{ce} = \frac{(M_{max}(\varphi_{ce}) - M)b}{M + a_{rel}M_{max}} \quad (1)$$

Here, ω_{ce} is the angular velocity of CE, M the CE moment, and $M_{max}(\varphi_{ce})$ the maximal moment CE can exert at this angle due to the moment-angle relationship. The shape of the moment-angular velocity relationship is determined by the dimensionless parameter a_{rel} and the parameter b[rad/s], which may also be expressed as $b_{rel} \equiv b/\varphi_{ce,opt}$ [Hz]. The active state q of CE is determined by the excitation dynamics, which will be described in Sec. 2.1.2.

SEE. This behaviour is characterized by its moment-extension relationship, which is modeled as a parabola:

$$M_{see} = k_{see}(\varphi_{see} - \varphi_{see,0})^2 \quad (2)$$

Here, M_{see} is the moment exerted by SEE, k_{see}[Nm/rad^2] the angular stiffness constant of SEE and $\varphi_{see,0}$[rad] the slack angle of SEE (i.e. the largest angle of SEE for which moment equals zero).

PEE. This moment also depends quadratically on PEE extension. Parameters are the PEE angular stiffness constant k_{pee}[Nm/rad^2] and PEE slack angle $\varphi_{pee,0}$[rad].

2.1.2 Excitation dynamics

Excitation dynamics is modeled as described by Hatze (1977, 1981). It consists of two parts. The first describes the calcium dynamics within the muscle and consists of two steps: (i) the neural excitation $\alpha(t)$ of the muscle fibres spreads inward along the T-tubuli, leading to a depolarization $\beta(t)$ of these tubuli; (ii) due to this depolarization, Ca^{2+} is released from the sarcoplasmic; reticulum, leading to an increase of the intracellular Ca^{2+} concentration $\gamma(t)$.

The second part of the excitation dynamics relates the intracellular Ca^{2+} concentration $\gamma(t)$ to the active state q of the muscle, which is defined as the relative amount of Ca^{2+} bound to troponin (Ebashi and Endo 1968). This part will be referred to as the active state-calcium relationship. Appendix A gives a detailed description of the model of muscle excitation used.

The MTC model is described by a set of five coupled differential equations which are solved by numerical integration using a variable order-variable step size integrator (Shampine and Gordon 1972). Inputs to the model are MTC angle and stimulation rate. Output includes, among other variables, the moment exerted by the muscle, which may be calculated from state variables.

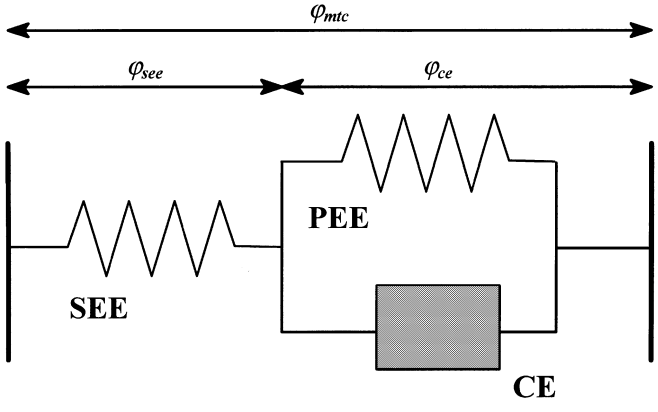

Fig. 1. Arrangement of the contractile element (*CE*), the series elastic element (*SEE*) and the parallel elastic element (*PEE*) with respect to each other. The angles used in this study are indicated. Note that in all cases, PEE angle equals CE angle

2.2 Human experiments

2.2.1 Subjects and experimental protocol

Four healthy subjects participated in this study. Informed consent was obtained from all subjects according to the policy statement of the American College of Sports

Medicine. The characteristics of the group were (mean ± standard deviation): age 25 ± 2 years, height 1.81 ± 0.06 m, body mass 71 ± 11 kg. All subjects participated in two separate experiments on the triceps surae (TS) muscle of their right leg. The first experiment was designed to determine the contractile properties of this muscle group, while data obtained in the second experiment were used to evaluate the performance of the excitation dynamics in describing the excitation of the TS muscle.

2.2.2 First experiment

In order to estimate the contractile properties of TS, each subject performed voluntary contractions on a special-purpose isokinetic dynamometer (Hof 1997a). With this dynamometer high angular velocities can be obtained, up to 20 rad/s, which are constant over a large range of motion. During experiments, the subject stood erect, with his right foot fixed to the dynamometer by means of a rigid polyurethane foam cast (Weiss et al. 1984). A series of isokinetic release contractions was performed on the TS muscle. In these contractions, the subject performed a maximal voluntary contraction (MVC) of TS, while the dynamometer was kept isometric. Once a constant isometric level of moment had been reached, the dynamometer was released and moved at a constant angular velocity, after a short acceleration phase. Isokinetic releases were performed at angular velocities ranging between approximately 2 rad/s and 15 rad/s. During all releases, the plantar flexion moment exerted by TS and the ankle joint angle were simultaneously sampled at 2000 Hz. The recorded moment was corrected for inertia by means of a special calculation method (Hof 1997b) and for passive antagonist moment. Since the muscle was activated voluntarily during this experiment, other plantar flexors besides TS could also have contributed to the recorded plantar flexion moment. However, cadaver data from Klein et al. (1996) indicate that these muscles (i.e. m. peroneus longus, m. peroneus brevis, m. tibialis posterior and m. flexor hallucis longus) have an average moment arm with respect to the ankle joint of about 1.43 cm, which is 3.5 times smaller than that of TS. Besides this, they have a total cross-sectional area which is about half that of TS, as can be derived from the literature review by Yamaguchi et al. (1990). Therefore, the contribution of these muscle to the plantar flexion moment can be estimated to be at best 1/7 of that of TS.

2.2.3 Second experiment

In order to evaluate the performance of the excitation dynamics, electrically evoked isometric contractions were performed on TS at different frequencies of stimulation. TS was artificially stimulated using a computer controlled stimulator identical to the one described by Prochazka et al. (1997). Using this device, TS was stimulated through the n. tibialis in the popliteal fossa, and the plantar flexion moment was recorded on a Kincom isokinetic device (Chattecx Corp., Chattanooga, TN), operating in isometric mode. Responses were elicited in TS by means of cathodal stimulation using a pen electrode with a surface area of 0.5 cm^2. The anode of 20 cm^2 was located 20 cm proximal of the stimulation site. The tibial nerve was stimulated using current pulses of 0.1 ms duration. During pilot experiments it was found that the mechanical response of the calf muscles to nerve stimulation depended strongly on the orientation of the electrode with respect to the nerve and to the pressure applied to the electrode. Therefore, it was found necessary to standardize the electrode position and pressure during each experiment. This was achieved by using an electrode holder, similar to the one described by Simon (1962), fixed to the leg by means of elastic bandages.

During experiments, the subject lay prone with his knee fully extended. The axis of his ankle joint was carefully aligned with the axis of rotation of the dynamometer. The ankle was positioned in a slightly plantarflexed position (100 deg, angle between the tibia and the sole of the foot). Next, using a low level of current of about 20 mA, the electrode position with respect to n. tibialis was determined at which the largest twitch response in TS was elicited. Subsequently, the stimulation current was raised until the twitch amplitude was at least 12 Nm. This usually required currents between 30 and 60 mA. Finally, a series of isometric contractions was elicited in which the stimulation frequency was increased up to the highest frequency which could be tolerated by the subject. In these contractions, TS was stimulated for 1 s. The moment exerted by TS, joint angle and stimulation synchronization pulses were simultaneously sampled at 1000 Hz and stored for subsequent analysis.

The impulse response of the footrest of the Kincom dynamometer was determined in a separate experiment. In this experiment, brisk ticks were applied to the footrest and the resulting moment transients recorded. An accelerometer was used to determine the exact instant of impact.

2.3 Determination of parameter values

2.3.1 Contraction dynamics

CE. The CE moment-angular velocity and SEE moment-extension relationships can be simultaneously derived from a set of isokinetic release contractions, provided that the set contains a release at such a high velocity that the moment eventually drops to zero. An efficient way to do this is by means of a self-consistent calculation (SCC), as proposed by Van Zandwijk et al. (1997a, b). In this method, the CE moment-angular velocity relationship is calculated from isokinetic release contractions at different angular velocities. The SEE moment-extension relationship is derived from the release at the highest angular velocity (i.e. the one in which the moment eventually drops to zero), a technique often referred to as the controlled release technique (i.e. Hill 1950; Hof 1997a).

In the isokinetic release contractions, the moment continuously decreases during the release. This implies that besides CE, SEE is shortening also. Therefore, the velocity of shortening of the MTC, i.e. the velocity by which the insertion approaches the origin, is divided among CE and SEE. In order to derive the CE moment-angular velocity relationship from such contractions, one needs to calculate the angular velocity of CE from the MTC angular velocity, i.e. estimate the SEE angular shortening velocity. This can be done by means of

$$\omega_{ce} = \omega_{mtc} + \frac{(dM/dt)}{2\sqrt{Mk_{see}}} \tag{3}$$

where ω_{ce} is the angular velocity of shortening of CE, ω_{mtc} the angular velocity of shortening of the MTC, M the moment exerted by TS, and k_{see} the angular stiffness constant of SEE.

In a controlled release experiment, a displacement is imposed on the MTC, and the moment is recorded. During the release, the moment drops below the isometric level. Therefore, CE will be able to shorten and take up some of the imposed displacement. The remainder is taken up by SEE. Hence, in order to obtain the SEE moment-extension relationship, one must allow for the amount of displacement taken up by CE by means of

$$\Delta\varphi_{see} = \Delta\varphi_{mtc} - \int_0^{t_f} \omega_{ce} dt = \Delta\varphi_{mtc} - \int_0^{t_f} \frac{(M_{init} - M)b}{M + a_{rel}M_{init}} dt \tag{4}$$

Here, $\Delta\varphi_{see} \equiv \varphi_{see} - \varphi_{see,0}$ is the stretch of SEE, $\Delta\varphi_{mtc}$ the angular displacement imposed on the MTC, and t_f the time at which $\Delta\varphi_{mtc}$ is attained, counted from the start of the release. M_{init} is the isometric moment before the start of the release. Note that the SEE angular stiffness constant k_{see} appears in (3) and that the CE moment-angular velocity parameters a_{rel} and b appear in (4). Therefore, the CE moment-angular velocity and SEE moment-extension relationship are mutually dependent when derived from isokinetic release contractions.

SCC determines those CE moment-angular velocity and SEE moment extension relationships which give a self-consistent description of the set of isokinetic releases. This means that they have the properties of (i) when the isokinetic releases are corrected for non-zero SEE velocity using the SEE moment-extension relationship, the CE moment-angular velocity relationship is obtained; and (ii) when the controlled release is corrected for CE shortening using the CE moment-angular velocity relationship, the SEE moment-extension relationship is obtained. It was demonstrated in Van Zandwijk et al. (1997a,b) that for isolated skeletal muscle, SCC yields a CE force-velocity and SEE force-extension relationship which are virtually identical to the ones obtained from a set of *isotonic* release experiments performed on the same muscle.

The moment-angle relationship of CE was estimated on the basis of the averaged number of sarcomeres found in fibres of the gastrocnemius muscle of four cadaver legs (Huijing, personal communication). Under the assumption that all fibres in parallel to each other contain the same number of sarcomeres, the optimum CE angle $\varphi_{ce,opt}$ can simply be calculated from the average number of sarcomeres found in the fibres multiplied by the optimum sarcomere length. The average number of sarcomeres found in m. gastrocnemius amounted to 17 825, which yields, after scaling for ratios of lower leg lengths, in combination with a value of human sarcomere optimum length of 2.94 μm (Walker and Schrodt 1974), a value of 1.2 rad for TS $\varphi_{ce,opt}$ and a value of 0.56 for w, which was used for all subjects. For each subject, the maximal isometric moment M_{max} was set to the moment reached during the plateau phase at the highest stimulation frequency tolerated by that subject.

SEE. As explained above, the SEE moment-extension relationship, and therewith the SEE angular stiffness constant k_{see}, was derived from an isokinetic release contraction at a high angular velocity, together with the CE moment-angular velocity relationship. The SEE slack angle $\varphi_{see,0}$ was adjusted so that CE is at $\varphi_{ce,opt}$ when exerting M_{max}, when the MTC is held at the test angle.

PEE. In the isometric contractions studied, the passive moment was negligible. Therefore, the PEE contribution was neglected by setting its angular stiffness constant k_{pee} to zero.

2.3.2 Excitation dynamics

Parameters in the excitation dynamics of the muscle model were estimated by minimization of a least squares objective function

$$\Phi(\theta) = \sum_i ((M_{exp}(t_i) - M_{cal}(\theta, t_i))^2 \tag{5}$$

with respect to the vector of parameters θ, describing the excitation dynamics. $M_{exp}(t_i)$ and $M_{cal}(\theta, t_i)$ are experimentally recorded and simulated muscle moment at time t_i, respectively. The numerical techniques used to minimize the objective function $\Phi(\theta)$ have been described extensively in Van Zandwijk et al. (1996). In short, the objective function $\Phi(\theta)$ is minimized by a Levenberg-Marquardt algorithm. This technique requires both the value of the objective function $\Phi(\theta)$ and its derivative with respect to the parameters θ to find iteratively those parameters minimizing $\Phi(\theta)$. This derivative was computed from so-called sensitivity equations which were integrated in parallel to the original model equations (Bard 1974).

Secondly, parameter values for the simplified version of the excitation dynamics were derived by fitting the Ca^{2+} response of the simplified model to the Ca^{2+} histories $\gamma(t)$ generated by the optimized excitation dynamics at a stimulation frequency of 100 Hz (cf Appendix A and Hatze 1977, 1981).

3 Results

3.1 Human experiments

3.1.1 First experiment

Figure 2 gives a typical example of an isokinetic release contraction performed on a human TS MTC at an angular velocity of 12 rad/s. Shown are raw data as well as data obtained by making corrections for inertia (cf Hof 1997b) and passive antagonist moment. Note that inertial transients at the start and stop of the release are much reduced by the correction method. Figure 3 shows the moment histories for a set of isokinetic release contractions performed at angular velocities of 3, 5, 10 and 15 rad/s after these have been corrected for inertia and passive antagonist moment. The latter velocity of release is sufficiently high to make the moment eventually drop to zero. For each release velocity, a similar behaviour of the muscle moment is observed. After an initial isometric phase, it drops rapidly at the onset of the release, the small ripple at the onset being a remainder of the inertial artefact. Finally, it drops steadily during the isokinetic phase of the release. The hump at the end of the release is again a remainder of the inertial artefact (cf Fig. 2). The lower panel shows electromyographic (EMG) time histories recorded from m. soleus for the releases shown in the upper panel. Note that the EMG amplitude is more or less constant during the release, the most important changes occurring at the end of the release. Figure 4 shows for the same subject the SEE moment-extension and CE moment-angular velocity relationship as calculated from the isokinetic release contractions by means of SCC. Note that for the CE moment-angular velocity relationship the correction for non-zero SEE velocity increases with velocity of shortening because of the increase in dM/dt (cf Fig. 3). For all subjects, the maximal angular velocity of shortening of the TS CE is approximately 10 rad/s, which is in agreement with earlier estimates of Hof and Van den Berg (1981). Table 1 summarizes for all subjects the parameters describing the contraction dynamics of the MTC model of TS.

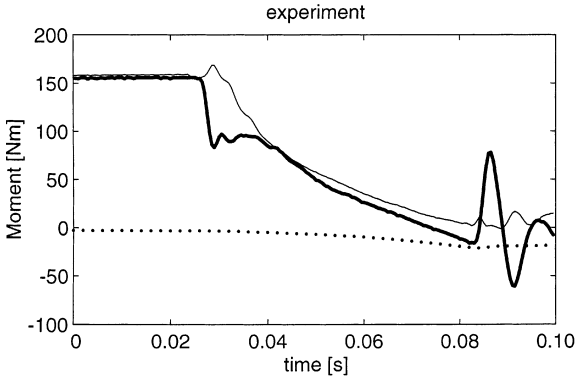

Fig. 2. Example of an isokinetic release contraction histories at a velocity of 12 rad/s. Shown are uncorrected data (*thick line*) and data obtained by making corrections for inertia and passive antagonist moment (*thin line*). The passive antagonist moment is shown by the *dotted line*. Note that the inertial transients at the start and end of the release are much reduced by the correction method (cf Hof 1997b)

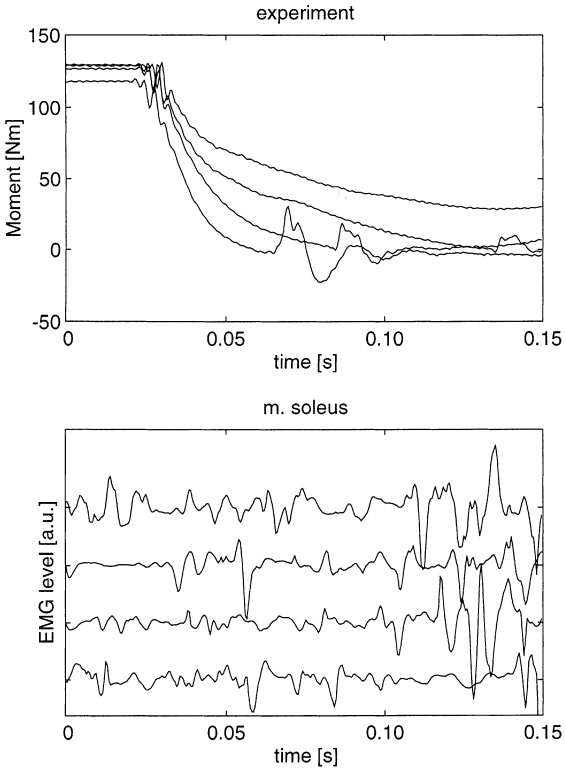

Fig. 3. *Top*: Typical example of isokinetic release contractions performed on a human triceps surae (TS) muscle for subject 1. Moment histories at velocities of shortening of approximately 3, 5, 10 and 15 rad/s (*from top to bottom*). During the release, the angular velocity decreases slightly (cf Hof 1997a). Data have been corrected for inertia and passive antagonist moment. The small ripple at the onset of the release is a remainder of an inertial transient, as are the humps at the end of the release (cf Fig. 2). *Bottom*: Electromyographic time histories recorded from m. soleus during the releases shown above at velocities of about 3, 5, 10 and 15 rad/s (from top to bottom). The same scale is used for all traces. Not all releases used as input for the self-consistent calculation are shown

3.1.2 Second experiment

Figure 5 gives a typical example of moment histories recorded during the electrically elicited isometric contractions. Shown are superimposed moment histories at different frequencies of stimulation. Typically, fused tetanic contractions were achieved at a stimulation frequency of 20 Hz. Note the decline of moment during the contraction, which is larger at low frequencies of stimulation. This effect will be addressed further in the Discussion. The maximal moment obtained in these electrically elicited contractions was in most cases lower than that achieved during a MVC at the same ankle angle. This indicates that not all motor units were recruited during electrical stimulation. Although the use of the electrode holder provided good stability and reproducibility of mechanical responses at low frequencies of stimulation, it remained difficult in a few cases to obtain such results at high frequencies of stimulation,

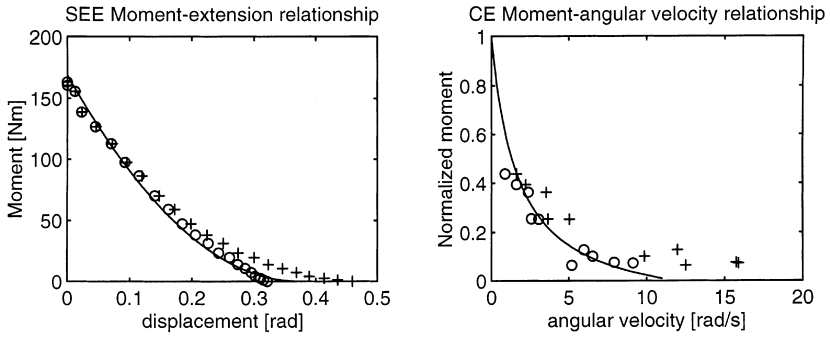

Fig. 4. SEE moment-extension and CE moment-angular velocity relationships for subject 1 as derived from the set of isokinetic releases by a self-consistent calculation (SCC). Shown are experimental data points (+) and points obtained by applying Eqs. (1) and (2) to the data (○), using those SEE moment-extension and CE moment-angular velocity relationships which yield the final, self-consistent description of the set of isokinetic releases. *Solid lines* are the fits to the models used to describe both relationships. For the CE moment-angular velocity relationship, all data points pertain to the same CE angle. *Left:* SEE moment-extension relationship *Right*: CE moment-angular velocity relationship

presumably due to increased bulging of m. gastrocnemius at these frequencies, leading to displacement of structures within the popliteal fossa. In the subsequent impulse response experiment it was found that the rise time of the moment transient due to brisk ticks applied to the footrest of the Kincom dynamometer was on average 6 ms. This is much lower than the rise times of muscle moment observed in the isometric experiments (cf Fig. 5). Therefore, the contribution of foot fixation to the rate of moment development is negligibly small.

3.2 Numerical experiments

Using the contraction dynamics as defined by the parameters in Table 1, parameters pertaining to the excitation dynamics were optimized for a single isometric twitch by minimization of the objective function (5). Figure 6 gives an example of measured as well as calculated twitch moment histories generated by the model after optimization of the parameters. The values of the parameters corresponding to the simulation shown in Fig. 6 are given in Table 2. Subsequently, the performance of this optimized excitation dynamics in predicting moment histories at other frequencies of stimulation was evaluated. The top panel of Fig. 7 shows for the same subject as in Fig. 6 predictions of moment histories at other stimulation frequencies, as well as measured moment histories. Similar results were obtained for all subjects, as is indicated by the lower panel of Fig. 7. This panel shows, for another subject, the measured as well as calculated moment histories obtained after parameters pertaining to the excitation dynamics were optimized for an isometric twitch. From Fig. 7 it is apparent that the optimized excitation dynamics provides encouragingly good predictions of isometric moment histories, albeit the moment is underestimated at higher stimulation frequencies. Finally, Fig. 8 compares for all subjects the peak moments obtained in the electrical stimulation experiment to those obtained in the model calculations, averaged over stimulation frequencies of 4, 8, 12, 16 and 24 Hz. Parameter values for the simplified version of the excitation dynamics were derived by fitting Ca^{2+} histories of the simplified model to those generated by the optimized excitation dynamics at a stimulation frequency of 100 Hz. These are given in Table 3 for all subjects. The value of the parameter m, which describes the rate of change of the Ca^{2+} concentration in the simplified model (cf Appendix A), falls for all subjects within the range given by Hatze (1977, 1981).

Table 1. Parameters describing the contraction dynamics of the human triceps surae muscle, obtained on the basis of isokinetic release contractions using SCC as well as on the basis of morphological data. The abbreviations used are explained in the main text

	Subject 1	Subject 2	Subject 3	Subject 4
k_{see} [Nm/rad^2]	1101	500	377	526
$\phi_{ce,opt}$ [rad]	1.2	1.2	1.2	1.2
M_{max} [Nm]	70	116	52	85
a_{rel}	0.13	0.23	0.21	0.30
b_{rel} [Hz]	1.37	2.15	1.55	2.97

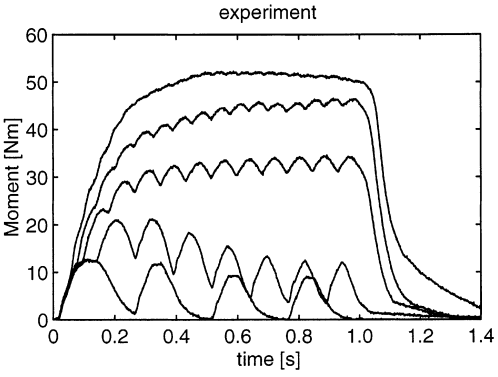

Fig. 5. Typical example of isometric moment histories, elicited in TS by electric stimulation of the tibial nerve for subject 3. Shown are moment histories at stimulation frequencies of 24, 16, 12, 8, and 4 Hz from top to bottom. Note the rapid decline of moment at low frequencies of stimulation

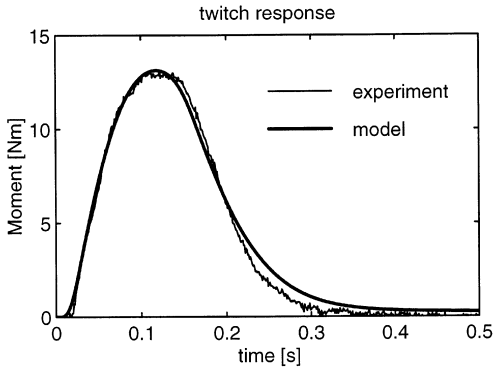

Fig. 6. Moment histories for both simulated and experimentally measured isometric twitches for subject 3. *Thin line* pertains to the experimentally measured twitch moment, and the *thick line* to moment generated by the model. The simulated twitch is obtained by optimization of the parameters pertaining to the excitation dynamics

3.3 Rate of change of moment during an isometric contraction

Figure 9 compares for all subjects simulations of moment development during maximally activated isometric plantar flexion. For comparison, a moment history calculated using parameter values for both contraction and excitation dynamics used previously for simulating the push-off in vertical jumping (Van Soest and Bobbert 1993) is shown as well. In the following, these parameter values will be called the original parameter values, in contrast to the new parameter values, as derived in this study for both the contraction- and excitation dynamics. In order to quantify the rate of change of variables, we calculated rise times (RTs). The RT of a variable is defined as the time required for that variable to rise from 10% to 90% of its maximal value. Under the condition of maximal activation (active state $q \equiv 1$), the RT of moment amounted to 30 ms for the original parameter values of the contraction dynamics. Under the same condition, the RT of moment amounted on average to 200 ms using parameter values of the contraction dynamics, as determined for the four subjects. Subsequently, we determined the RT of the active state q for the simplified version of the model of excitation. This RT obviously depends on the level of stimulation used. Therefore, the RT of the active state was determined for a low and a high level of stimulation and averaged. For the original parameter values of the excitation dynamics, this averaged RT of active state was 100 ms. Using the excitation dynamics derived on the basis of experimental data of the four subjects, the RT of the active state was found to be 142 ms on average, under the same conditions.

Table 2. Parameter values describing the excitation dynamics for subject 3, after optimization for an isometric twitch. The meaning of the parameters is explained in Appendix A. For each parameter, the 95% confidence interval is given in parentheses

Parameter	
θ_1	3.50×10^5 $(2.92 \times 10^5 - 3.99 \times 10^5)$
θ_2	5.58×10^6 $(4.43 \times 10^6 - 5.87 \times 10^6)$
θ_3	1.85×10^4 $(9.9 \times 10^3 - 7.07 \times 10^4)$
θ_4	2.92×10^5 $(1.53 \times 10^5 - 1.25 \times 10^6)$
θ_5	4.57×10^{14} $(2.52 \times 10^{14} - 1.96 \times 10^{15})$

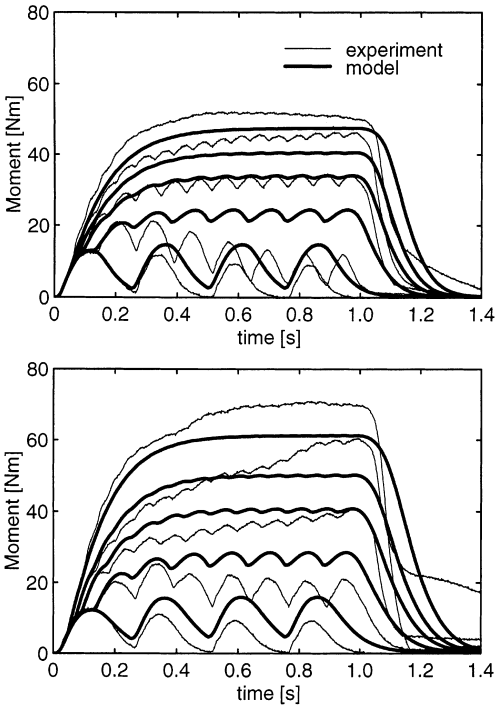

Fig. 7. Isometric moment histories for subjects 3 (*top*) and 1 (*bottom*) at different frequencies of stimulation. In each panel, *thin lines* pertain to experimentally recorded muscle moment, while *thick lines* pertain to muscle moments generated in the model calculations. For both the experimental and simulated moment histories, the *uppermost trace* corresponds to a stimulation frequency of 24 Hz and *subsequent traces* to frequencies of 16, 12, 8 and 4 Hz, respectively. The simulated moment histories have been calculated using the values of the parameters describing the excitation dynamics, obtained by optimization of model behaviour for an isometric twitch, i.e. the data shown in Fig. 5 for the top panel. Note that relaxation is slower in the model than in the experiment

4 Discussion

The purpose of this research was to investigate the extent to which a model of muscle excitation which linearly sums responses to individual stimuli can describe the excitation of human muscle in vivo. To this end, values of parameters describing the contractile behaviour of human TS muscle were determined on the basis of voluntary isokinetic release contractions and morphological data. Next, parameters pertaining to the excitation dynamics were optimized such that moment histories during an isometric twitch were correctly predicted. Finally, it was evaluated whether this optimized model was capable of predicting moment histories at other stimulation frequencies.

We estimated the contractile properties of TS on the basis of a set of voluntary isokinetic release contractions.

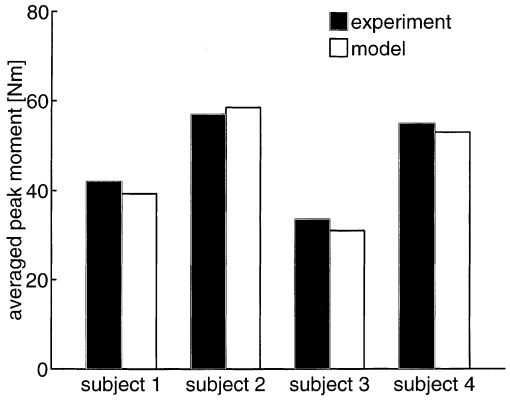

Fig. 8. Averaged peak moments attained in both the experimentally recorded and calculated isometric contractions for all subjects. Moments are averaged over frequencies of 4, 8, 12, 16 and 24 Hz

Therefore, the question can be raised of whether muscle activation varied from trial to trial and whether it remained constant during the releases. As far as the first point is concerned, the subjects were instructed to exert a prescribed plantar flexing moment before the dynamometer was released. For that reason, the variation in initial moment is quite small, as can be seen from Fig. 3. The fastest releases are completed well within 50 ms, which is about the time at which the fastest reflexes arrive. Therefore, it seems unlikely that muscle stimulation, let alone the active state has changed appreciably during these releases. For releases at lower velocities, however, there might be enough time to adjust muscle stimulation during the release. EMG signals recorded from m. soleus (Fig. 2) indicate that the largest changes in EMG amplitude occur after the release has been completed and therefore provide some confidence that muscle stimulation and the active state remained constant during the releases.

The results shown in Fig. 7 indicate that this model of muscle excitation does indeed give a reasonable description of the processes involved in the excitation of human TS muscle. Therefore, it appears that a model which sums responses to stimulation pulses linearly and calculates the active state of the muscle from these responses by means of a non-linear transformation can be useful in describing the processes involved in the excitation of human muscle. Unfortunately, however, a number of marked differences remain between the model predictions and experimental data. For instance, as can be seen from Fig. 7, relaxation is much slower in the model than in the experiment. Also, the model is unable to predict the decline of moment at low frequencies of stimulation. Changes in twitch amplitude during stimulation at low rates have been known for a long time in both skeletal and cardiac muscle and are usually referred to as staircase phenomena. Staircase phenomena can be either positive (successive twitches increase in amplitude) or negative (successive twitches decrease in amplitude). For human adductor pollicis muscle in vivo, Desmedt and Hainaut (1968) found an initially negative staircase, followed by a prolonged positive staircase. For isolated cat muscle, Parmiggiani et al. (1982) found prolonged positive staircases for fast m. plantaris and prolonged negative staircases for slow m. soleus. According to these authors, the nature of the processes underlying these phenomena is unknown, but they are most likely due to slow changes in the Ca^{2+} dynamics during contraction. Such processes have not been incorporated in the present model. Therefore, it is not surprising that it is unable to predict the negative staircase observed in our TS stimulation experiments at low frequencies of stimulation.

Currently, it is difficult to compare the performance of this model to that of other models, since for many other models, data which directly compare experimental data and model predictions are not available in the literature. Riener et al. (1996), Riener and Quintern (1997) are among the few who qualitatively evaluated their model of excitation and contraction dynamics of human muscle using experimental data. They found that their model, parts of which are based on the same model as used in this study (Hatze 1977), could reproduce many characteristics of artificially stimulated muscle. For the model of human muscle excitation proposed by Khang and Zajac (1989), parameters are adjusted to approximate moment histories in an isometric twitch, but performance in predicting tetanic muscle moments was not evaluated.

Comparison between parameter values obtained in this study and those used previously to simulate the push-off phase in vertical jumping (i.e. Van Soest and Bobbert 1993) revealed large differences in the speed of the contraction dynamics (cf Fig. 9). The contraction dynamics as determined on the basis of experimental data from human muscle is about 7 times slower than the contraction dynamics used in that study, which was derived on the basis of data from isolated skeletal muscle from the literature. On the other hand, the excitation dynamics as determined from the electrical stimulation experiments was on average only 42% slower than that used in the latter study. So, for isometric plantar flexion,

Table 3. Parameter values describing the first-order trend function for all subjects. The meaning of the parameters is explained in Appendix A. Parameter values were derived by fitting the model (9) to Ca^{2+} histories $\gamma(t)$ generated by the optimized excitation dynamics at a stimulation frequency of 100 Hz. For each parameter, the 95% confidence interval is given in parentheses. Note that these intervals are much smaller than for parameters describing the complex model (cf Table 2)

	Subject 1	Subject 2	Subject 3	Subject 4
m	6.54 (6.41–6.56)	8.52 (8.49–8.53)	7.94 (7.90–7.96)	5.06 (5.04–5.07)
c	1.36×10^{-4} (1.35×10^{-4}–1.37×10^{-4})	1.10×10^{-4} (1.10×10^{-4}–1.11×10^{-4})	1.57×10^{-4} (1.56×10^{-4}–1.57×10^{-4})	1.83×10^{-4} (1.82×10^{-4}–1.83×10^{-4})

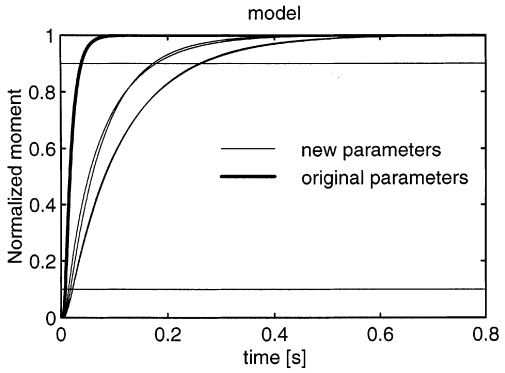

Fig. 9. Simulated moment histories for maximally activated plantar flexion using parameter values for the contraction dynamics as defined in Table 1 for the four subjects (*thin lines*). A simulation using the contraction dynamics used previously for simulating the push-off phase in vertical jumping (Van Soest and Bobbert 1993) is shown for comparison by the *thick line*. To facilitate comparison among subjects, moment histories are normalized with respect to their maximal values. The rise time (RT) of the moment histories is the time required by the signals to rise from 10% to 90% of their maximal value, i.e. from the bottom horizontal line to the top horizontal line

the excessively fast rise of moment can to a large extent be attributed to the contraction dynamics of the model used being too fast and to a much lesser extent to the excitation dynamics used being too fast. In order to assess the contribution of stimulation dynamics to force development, simulation of muscle contractions using electromyograms as input seem to be indicated. These will be the subject of a subsequent paper.

Acknowledgements. Technical assistance by W. Engel and K. Noppe is gratefully acknowledged. We thank Drs. T. de Haan for assistance during data acquisition. We are indebted to an anonymous reviewer for useful comments on the manuscript.

Appendix
Details of the model of muscle excitation

Following Hatze (1977, 1981), the excitation dynamics of the contractile element of the muscle is described by two second-order differential equations:

$$\frac{d^2\beta}{dt^2} + \theta_i \frac{d\beta}{dt} + \theta_2\beta = \alpha(t) \tag{6}$$

$$\frac{d^2\gamma}{dt^2 t} + \theta_3 \frac{d\gamma}{dt} + \theta_4\gamma = \beta(t) \tag{7}$$

Here $\alpha(t)$ is the neural control signal, $\beta(t)$ the depolarization of the T-tubuli, and $\gamma(t)$ the free intracellular Ca^{2+} concentration as described in the main text. When driven by a single pulse for $\alpha(t)$, the system (6)–(7) yields an asymmetrically shaped response for the intracellular Ca^{2+} concentration α(t), a fact which is also observed in experiments where intracellular calcium transients are recorded by means of calcium-sensitive dyes (i.e. Blinks et al. 1978).

Note that the system of (6)–(7) is linear in the driving term α(t) and that its output is determined by the value of parameters $\theta_1 - \theta_4$ and the shape of the neural control signal $\alpha(t)$. In this study we used a half-sine wave with a half-period of 1 ms for a single stimulation pulse. This means that when the model is stimulated at a frequency of e.g. 80 Hz, the neural control signal is given by

Table 4. Parameter values for the active state-calcium relationship

Parameter	
q_0	0.005
ρ_2	1.05
$\breve{\xi}$	2.90
s	1.0

$$\alpha(t) = \sin(1000\pi(t - t_0)), \quad t_0 < t < t_0 + 0.001, \qquad t_0 = \frac{n}{80},\ n \in N$$
$$\alpha(t) = 0 \quad \text{elsewhere} \tag{8}$$

The active state q of the contractile element is calculated from the free intracellular Ca^{2+} concentration $\gamma(t)$ by means of

$$q(\gamma, \xi) = 1 - \frac{1 - q_0}{m_1 - m_2}\left(m_1 e^{m_2\rho^*(\xi)\theta_5\gamma} - m_2 e^{m_1\rho^*(\xi)\theta_5\gamma}\right) \tag{9}$$

Here $m_{1,2} = -\rho_2 \pm \sqrt{\rho_2^2 - 1}$, where ρ_2 is a constant, ξ is the length of CE relative to $\phi_{ce,opt}$, and q_0 is a constant. The length dependence of the active state q is incorporated into (8) by means of the term

$$\rho^*(\xi) = \frac{\breve{\xi}^s - 1}{\left(\frac{\breve{\xi}}{\xi}\right)^s - 1}$$

where s and $\breve{\xi}$ are constants. The shape of the active state-calcium relationship (8) is determined by the value of the constants ρ_2, s, q_0 and $\breve{\xi}$. For details concerning the derivation of (9) as well as its underlying assumptions, the reader is referred to Hatze (1977, 1981). The parameters describing the excitation dynamics are θ_1–θ_5. These are the parameters which are optimized as explained in the main text. Parameter values determining the shape of the active state calcium relationship are summarized in Table 4.

When studying multi-segment movement control, the many structural details incorporated in the model of muscle excitation as described by (6)–(9) can be of minor importance. In those cases, the muscle excitation can be approximated by a first-order trend function, which describes the averaged behaviour of the more complex model (Hatze 1977, 1981).

This trend function is described by the first-order differential equation

$$\frac{d\gamma}{dt} = m(cv - \gamma) \tag{10}$$

where $\gamma(t)$ is the intracellular Ca^{2+} concentration, as before, v is the normalized stimulation rate of the muscle, and m and c are constants. Following Hatze, the stimulation frequency is normalized with respect to the maximal stimulation frequency of 100 Hz, which is taken by definition as $v \equiv 1$. Given the intracellular Ca^{2+} concentration, the active state q of CE is calculated using (9) or an approximation to this expression.

References

Bard Y (1974) Nonlinear parameter estimation. Academic Press, New York

Blinks JR, Rüdel R, Taylor SR (1978) Calcium transients in isolated amphibian muscle fibres: detection with aeqorin. J Physiol [London] 277:291–323

Bobbert MF, Zandwijk JP van (1994) Dependence of human maximal jump height on moment arms of the bi-articular m. gastrocnemius; a simulation study. Hum Movement Sci 13:697–716

Desmedt J, Hainaut K (1968) Kinetics of myofilament activation in potentiated contractions: staircase phenomena in human skeletal muscle. Nature 217:529–532

Ebashi S, Endo M (1968) Calcium ion and muscle contraction. Prog Biophys Mol Biol 18:125–183

Hatze H (1977) A myocybernetic control model of skeletal muscle. Biol Cybern 25:103–119

Hatze H (1981) Myocybernetic control models of skeletal muscle. University of South Africa, Pretoria

Hill AV (1938) The heat of shortening and the dynamic constants of muscle. Proc R Soc Lond [Biol] 126:136–195

Hill AV (1950) The series elastic component of muscle. Proc R Soc Lond [Biol] 137:273–280

Hof AL (1997a) A controlled-release ergometer for the human ankle. J Biomech 30:203–206

Hof AL (1997b) Correcting for limb inertia and compliance in fast ergometers. J Biomech 30:295–297

Hof AL, Berg JW van den (1981) EMG to force processing II: estimation of parameters of the Hill muscle model for the human triceps surae by means of a calf ergometer. J Biomech 14: 759–770

Khang G, Zajac FE (1989) Paraplegic standing controlled by functional neuromuscular stimulation. Part I. computer model and control-system design. IEEE Trans Biomed Eng 36:873–884

Klein P, Mattys S, Rooze M (1996) Moment arm length variations of selected muscles acting on talocrural and subtalar joints during movement: an in vitro study. J Biomech 29:21–30

Pandy MG, Zajac FE (1991) Optimal muscle coordination strategies for jumping. J Biomech 24:1–10

Pandy MG, Zajac FE, Sim E, Levine WS (1990) An optimal control model for maximum height human jumping. J Biomech 23:1185–1198

Parmiggiani F, Stein RB, Rolf R (1982) Slow changes and Wiener analysis of nonlinear summation in contractions of cat muscles. Biol Cybern 42:177–188

Prochazka A, Gautier M, Wieler M, Kenwell Z (1997) The bionic glove: an electrical stimulator garment that provides controlled grasp and hand opening in quadriplegia. Arch Phys Med Rehabi 78:608–614

Riener R, Quintern J (1997) A physiologically based model of muscle activation verified by electrical stimulation. Bioelectrochem and Bioenerg 43:257–264

Riener R, Quintern J, Psaier E, Schmidt G (1996) Physiologically based multi-input model of muscle activation. In: Pedotti A, Ferrarin M, Quintern J, Riener R (eds.) Neuroprosthetics. Springer Berlin Heidenberg New York

Shampine LF, Gordon MK (1972) Computer solution of ordinary differential equations: the initial value problem. WH Freeman, San Fransisco

Simon J-NM (1962) Dispositif de Contention des Électrodes de Stimulations pour l'Étude du Réflexe de Hoffmann chez l'Homme. Electroenceph Clin Neurophysiol [suppl] 22:174–176

Soest AJ van, Bobbert MF (1993) The contribution of muscle properties in the control of explosive movements. Biol Cybern 69:195–204

Walker SM, Schrodt GR (1974) Segment length and thin filament periods in skeletal muscle fibres of the rhesus monkey and the human. Anat Rec 178:63–82

Weiss PL, Hunter IW, Kearney RE (1984) Rigid polyurethane foam casts for fixation of human limbs. Med Biol Eng Compu 22:603–604

Yamaguchi GT, Sawa AGU, Moran DW, Fessler MJ, Winters JM (1990) A survey of human musculotendon actuator parameters. In: Winters JM, Woo SL-Y (eds) Multiple muscle systems. Springer, Berlin Heidelberg New York

Zandwijk JP van, Bobbert MF Baan GC, Huijing PA (1996) From twitch to tetanus: performance of excitation dynamics optimized for a twitch in predicting tetanic muscle forces. Biol Cybern 75:409–417

Zandwijk JP van, Baan GC, Huijing PA, Bobbert MF (1997a) How to obtain CE force-velocity and SEE force-extension relationships from isokinetic releases. Proceedings of the XVIth Congress of the International Society of Biomechanics, Tokyo

Zandwijk JP van, Baan GC, Bobbert MF, Huijing PA (1997b) Evaluation of a self-consistent method for calculating muscle parameters from a set of isokinetic releases. Biol Cybern 77:277–281